

AD-A114 206

NAVAL RESEARCH LAB WASHINGTON DC

F/G 18/1

INTERNAL HEAT DEPOSITION IN LASER HIGHLY-ACCELERATED TARGETS.(U)

APR 82 B H RIPIN, E A MCLEAN, J A STAMPER

DE-A108-79DP40092

UNCLASSIFIED

NRL-MR-4811

NL

1001



END
DATE
FILMED
5-82
DTIC

ADA11420C

SECURITY CLASSIFICATION OF THIS PAGE (When Data Entered)

REPORT DOCUMENTATION PAGE		READ INSTRUCTIONS BEFORE COMPLETING FORM
1. REPORT NUMBER NRL Memorandum Report 4811	2. GOVT ACCESSION NO. AD-A114206	3. RECIPIENT'S CATALOG NUMBER
4. TITLE (and Subtitle) INTERNAL HEAT DEPOSITION IN LASER HIGHLY-ACCELERATED TARGETS	5. TYPE OF REPORT & PERIOD COVERED Interim report on a continuing NRL problem.	
7. AUTHOR(s) B.H. Ripin, E.A. McLean and J.A. Stamper	6. PERFORMING ORG. REPORT NUMBER	
9. PERFORMING ORGANIZATION NAME AND ADDRESS Naval Research Laboratory Washington, DC 20375	8. CONTRACT OR GRANT NUMBER(s) DE-A108-79DP40092	
11. CONTROLLING OFFICE NAME AND ADDRESS U.S. Department of Energy Washington, DC 20545	10. PROGRAM ELEMENT, PROJECT, TASK AREA & WORK UNIT NUMBERS 47-0859-0-2	
14. MONITORING AGENCY NAME & ADDRESS (if different from Controlling Office)	12. REPORT DATE April 23, 1982	
	13. NUMBER OF PAGES 14	
	15. SECURITY CLASS. (of this report) UNCLASSIFIED	
	15a. DECLASSIFICATION/DOWNGRADING SCHEDULE	
16. DISTRIBUTION STATEMENT (of this Report) Approved for public release; distribution unlimited.		
17. DISTRIBUTION STATEMENT (of the abstract entered in Block 20, if different from Report)		
18. SUPPLEMENTARY NOTES This work was supported by the U.S. Department of Energy.		
19. KEY WORDS (Continue on reverse side if necessary and identify by block number) Laser plasma Heat flow Equation of state Laser fusion Plasma Preheat Fluid expansion		
20. ABSTRACT (Continue on reverse side if necessary and identify by block number) A novel method is described from which estimates of the internal pressure or temperature of highly accelerated material can be made. The technique is applied to Nd-laser ablatively accelerated targets and the results compare well with target rear surface temperature measurements using time-resolved optical pyrometry.		

DTIC
SELECTED
MAY 7 1982
FH

DD FORM 1473
1 JAN 73

EDITION OF 1 NOV 65 IS OBSOLETE
S/N 0102-014-6601

SECURITY CLASSIFICATION OF THIS PAGE (When Data Entered)

INTERNAL HEAT DEPOSITION IN LASER HIGHLY-ACCELERATED TARGETS

In inertial confinement fusion, a pellet containing fusible fuel, such as deuterium-tritium, is imploded by ablating material from the pellet surface with beams from an intense driver such as a laser or accelerator. One of the conditions to achieve a sufficiently high-density implosion is that the fuel not be prematurely heated above a few times the Fermi degenerate level during the implosion phase. There are several ways that preheat in laser irradiated targets have been inferred; these methods include: time-resolved optical pyrometry of target rear surfaces,¹ inferences from the distribution of fusion reaction products in pellet compression experiments,² spectroscopic observations of fast electron induced K_{α} -emission,³ and others. Time-resolved optical pyrometry, in which the target is assumed to emit light close to that of a blackbody in the spectral range of observations, has proven valuable in providing detailed temperature information of the rear surface of accelerated targets.¹ However, only temperatures from relatively low density material (several times $10^{20}/\text{cc}$) have been accessible with this technique due to the short optical depths of the visible emission. Hence, until now, the temperature of the denser material in the bulk of the accelerated targets has been only inferred through hydrodynamic computer calculations. Here, we describe a novel method to extract estimates of the internal pressure and temperature of dense accelerated targets; the results obtained using this method corroborate those inferred using optical pyrometry.^{1,4}

The new method exploits the initial free expansion properties of a fluid boundary which is suddenly released. When a bounded fluid (gas) is suddenly allowed to expand, as illustrated in Fig. 1, the material in the front edge of the boundary moves supersonically with velocity u . The initial expansion velocity is a simple function of the state properties of the fluid- which we wish to infer. We assume an adiabatic expansion model⁵ since the

Manuscript submitted March 5, 1982.

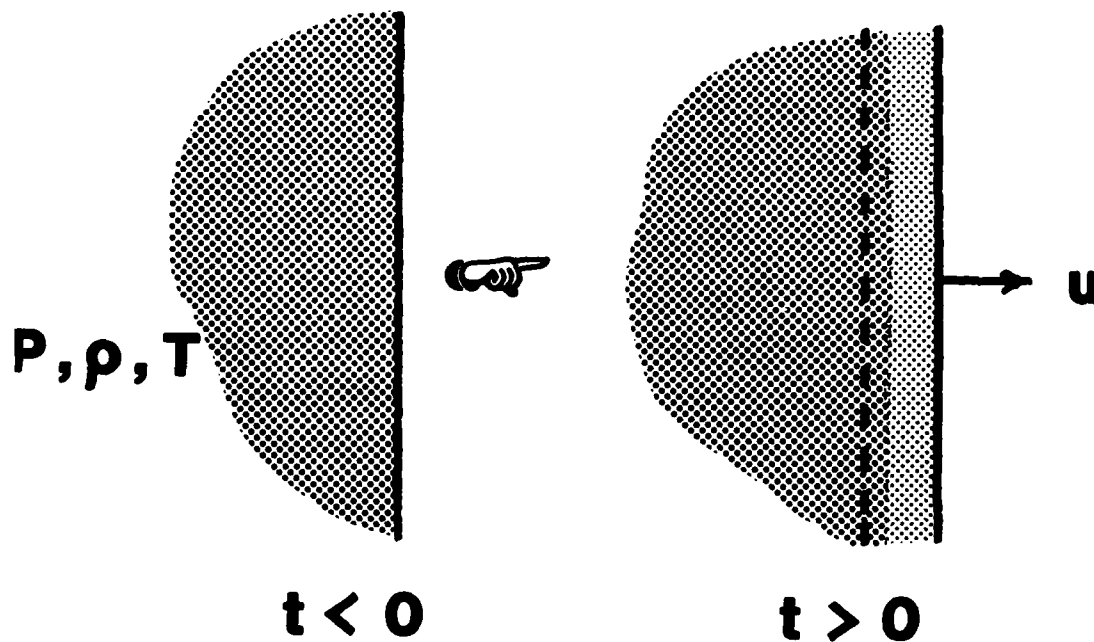


Fig. 1 — A fluid boundary that is suddenly released at $t = 0$ expands supersonically with velocity u . This principle can be used to infer state variables of the fluid.

Accession For	
NTIS GRA&I	<input checked="" type="checkbox"/>
DTIC TAB	<input type="checkbox"/>
Unannounced	<input type="checkbox"/>
Justification	
By _____	
Distribution/	
Availability Codes	
Dist	Avail and/or Special
A	



expansion is initially rapid and supersonic. Also, under most circumstances the heat load on the target has terminated at the time of observation; that is the laser pulse is over. Under these circumstances the fluid surface expands with velocity⁵

$$u = \frac{2}{\gamma-1} c_s, \quad (1)$$

where the sound speed c_s is related to the ratio of specific heats γ in the fluid, the fluid pressure P and the mass density ρ by $c_s^2 = \gamma P / \rho$. Thus, using $P = (Z + 1) \kappa T / A m_p$, where Z, A, T are the fluid ionization state, atomic number and temperature, and m_p and κ are the mass of the proton and the Boltzman constant, we find an approximate relationship between the observed fluid surface velocity and internal target temperature to be

$$\kappa T = \frac{A m_p}{Z+1} \frac{(\gamma-1)^2}{4\gamma} u^2. \quad (2)$$

This expression for temperature is independent of density (except implicitly in γ and Z), therefore the results are insensitive to the density of observation. The insensitivity of the expansion velocity to density is fortunate, for it allows the use of a rather simple expansion model for estimates of internal temperature without concern for details of the density profile of the target, or the need for a complex hydrodynamic calculation. On the other hand, the corresponding relation between u and internal pressure is

$$P = (\gamma-1)^2 \rho u^2 / 4, \quad (3)$$

which is explicitly a function of density.

A number of simplifying assumptions are incorporated into this model to apply it as an internal temperature diagnostic, these include: (i) ignoring the implicit density dependence of γ and Z , (ii) use of a constant value of

5/3 for γ , (iii) assuming an average internal temperature and (iv) using simple iterative estimates for Z . Despite the simplifications in the present model, the temperatures inferred are estimated to be accurate to $\pm 30\%$; this is significant because the measurements presented here are believed to be the first in the near solid density, low temperature regime, and are not easily accessible by other means. Better precision should be ultimately achievable if sophisticated hydrodynamic computer calculations are invoked. However, a major point in this paper is to show that, with laser-irradiated targets under our conditions, rear surface temperature measurements using optical pyrometry do give good estimates of the targets' internal temperatures; the present model suffices for this purpose.

The simple relationship between temperature and expansion velocity is exploited experimentally by placing a massive knife edge in the path of the accelerated targets, such as illustrated in Figure 2. The knife edge is termed a HA (half-aft) target. The freshly cut edge of the accelerated target, as it sweeps past the HA-target, expands perpendicular to the direction of motion. This lateral expansion of the target edge is observed using an optical streak camera (viewing the rear of the HA-target) and multiple-time optical interferometry or shadowgraphy (viewing edge-on to the targets). In our experiments the accelerated targets are moving supersonically with respect to both the sound speed within the target and the expansion front. Therefore, shock waves generated when the target is sheared off at the HA-target do not affect the expansion velocity. Simultaneously, throughout the acceleration period, time-resolved target rear-surface temperatures, T_r , are measured by using the two wavelength optical pyrometer described by McLean et al.¹ Note that the ionization state of the target is needed in Eq. 2 to infer its internal temperature; Z is obtained by

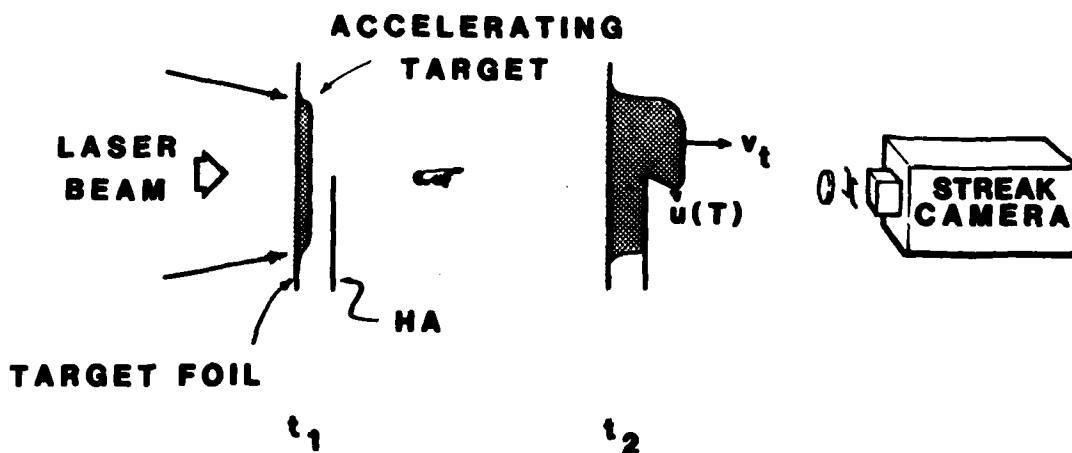


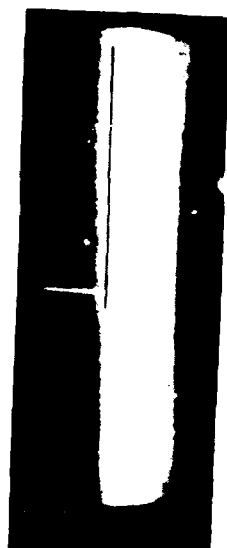
Fig. 2 — Experimental arrangement for accelerating a target to high speed, creating a sharp target boundary and diagnosing its evolution. The target velocity is v_t and the lateral expansion of the fluid edge, from which we infer the target internal temperature is u . An optical streak camera, whose slit is imaged vertically, monitors the expansion of the heated, visibly emitting target past the HA-target edge; the time-resolved optical pyrometer views the top half of the accelerated target from the same direction. The backlighting optical probe beam used for shadowgraphy is directed out of the plane of the paper through the target region; it thus monitors both u and v_t . The optical probe was $0.53 \mu\text{m}$ light of time duration less than 0.5 nsec .

referring to SESAME equation of state tables⁶ by first using T_r to obtain Z' , a first estimate for Z , inserting Z' in Eq. 2 to obtain a correction for T , and then iterating until convergence occurs. Usually only one or two iterations is necessary. The ratio of specific heats is assumed to be $\gamma = 5/3$ and the density assumed in the SESAME table lookup is 0.13 solid; variations of either variable do not appear to affect the results sensitively. It is noted that $\gamma = 5/3$ is appropriate for an ideal gas, Fermi degenerate plasma, and is nearly that found for the expansion of a fully ionized plasma front.⁷

The accelerated targets are typically a few microns thick Al or $(CH)_n$ foils irradiated over about 1-mm diameter with 3-nsec Nd-laser light at approximately 10^{13} W/cm^2 . The laser and its properties are described in detail in reference 8 and the experimental arrangement in reference 9. The HA-targets are 10 μm thick gold foils placed a few hundred microns behind the initial accelerated foil location and oriented with its edge approximately halfway into the path of the accelerated foil. Figure 3 shows two examples of the experimental results. In Fig. 3a the velocity of the cutoff edge of an aluminum target, whose directed velocity is $1 \times 10^7 \text{ cm/sec}$, is $u = 2 \times 10^6 \text{ cm/sec}$, or corresponding to about 7 eV temperature from Eq. 2; this value is comparable to the 11 eV peak rear surface temperature observed from optical pyrometry. The shadowgrams show the target before acceleration and 2 nsec after the peak of the acceleration laser pulse when the target is just impacting the HA-target, placed 270 μm behind the initial target location. The parameters in this example are typical of our target acceleration experiments.⁹ The second example, Fig. 3b, shows a lower mass accelerated $(CH)_n$ target which exhibits higher directed velocity and edge expansion velocity than did the first example. One can easily see the lateral expansion of the edge in the streak photograph and dual-time, dark-field

STREAK PHOTOGRAPH

$u = 2 \times 10^6 \text{ cm/sec}$
($T \approx 7 \text{ eV}$)

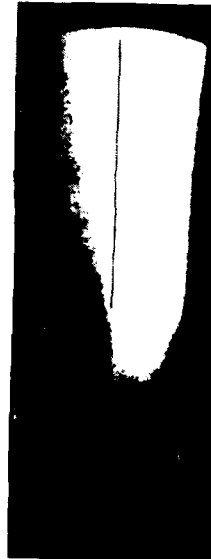


(a)

TIME (nsec)

STREAK PHOTOGRAPH

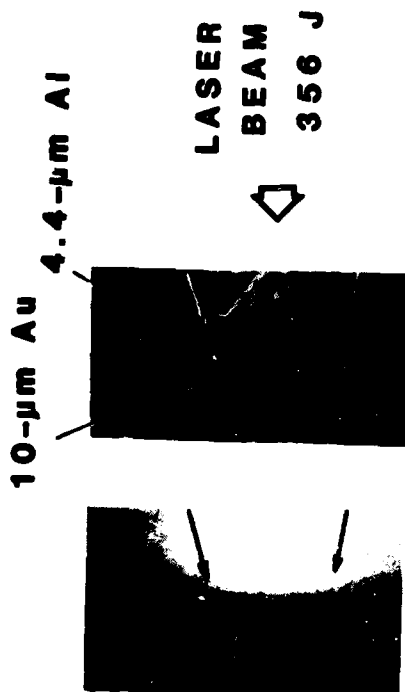
$u = 7 \times 10^6 \text{ cm/sec}$
($T \approx 18 \text{ eV}$)



(b)

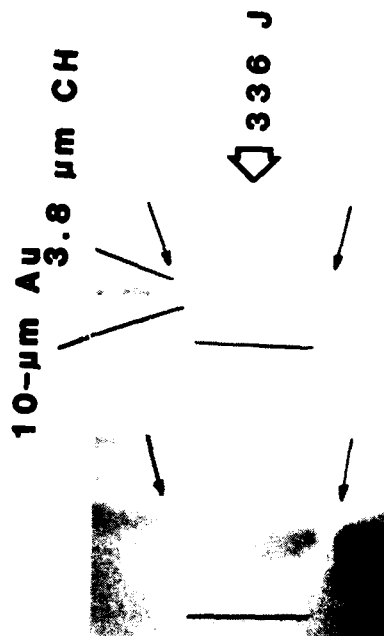
TIME (nsec)

SHADOWGRAMS HA-TARGET



$t = +2 \text{ nsec}$

DUAL-TIME, DARK-FIELD
SHADOWGRAM HA-TARGET



$t = +1, +2 \text{ nsec}$

Fig. 3 — Examples of data obtained in HA-target experiments. (a) Case of a $4.4 \mu\text{m}$ Al thick target achieving a velocity, v_t , of approximately $1 \times 10^7 \text{ cm/sec}$ interacting with a HA-target. (b) Case of a less massive $3.8 \mu\text{m}$ (CH)_n target accelerated to $v_t = 1.8 \times 10^7 \text{ cm/sec}$ which was heated to a greater degree than that of case (a).

shadowgrams; a $T = 18$ eV temperature was inferred from edge expansion which is again comparable to the 21 eV peak rear surface temperature observation. The dual-time, dark-field shadowgrams show the target boundary motion at +1 and +2 nanoseconds with respect to the peak of the laser pulse.

Comparison of the internal target temperatures inferred by using a HA target with corresponding peak rear surface temperatures is shown in Figure 4; a variety of $(CH)_n$ and Al target thicknesses and HA-target separation distances were used here. Note, that within experimental error the two methods agree. Although the closeness of this agreement may be somewhat fortuitious, since both methods rely upon a number of intermediate assumptions, it is reassuring that they both track and are of the same order.

The technique can be expanded to infer the target temperature at different times of the acceleration phase by varying the separation of the HA-target from the initial foil location. The measurement is then representative of the time at which the target is sheared off. Figure 5 shows an example which illustrates this point. The temperature of a thin (initially $3.8 \mu m$) $(CH)_n$ foil initially increases and then decreases with target separation. This behavior appears consistent with the observation that the thin fast target gets sheared off during the laser pulse for small separations where only a fraction of the total heat has been deposited, and hence a lower than peak temperature. At late times (large target separations) the temperature decreases due to adiabatic expansion cooling of target and radiative losses. The time of the peak temperature observation (+1.5 nsec), in fact, is consistent with the corresponding HA-target separation of about $275 \mu m$ and final target velocity of 1.8×10^7 cm/sec; it is also in agreement with the temperature-time characteristics published in reference 10.

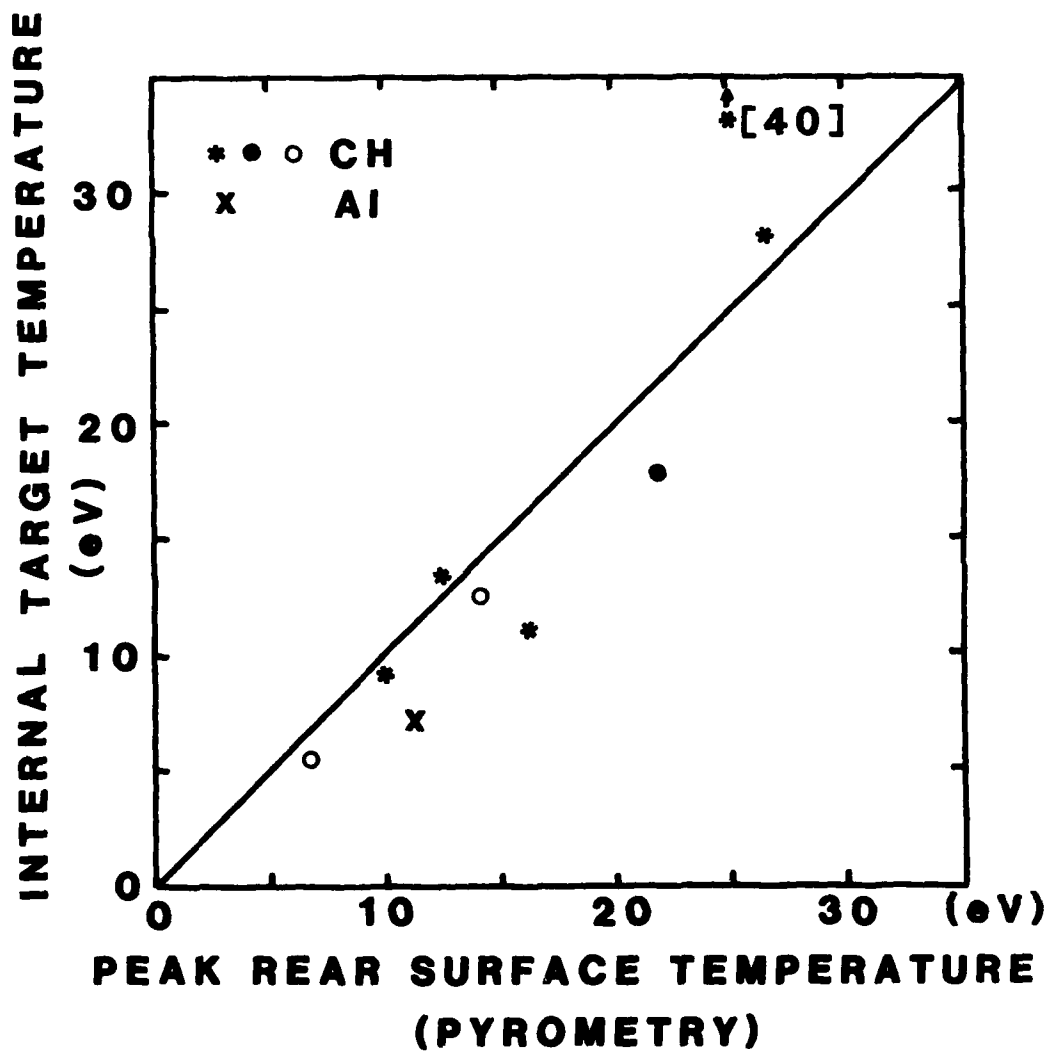


Fig. 4 — Comparison of the target internal temperature obtained with HA-targets with the observed peak rear surface temperature for a variety of targets.

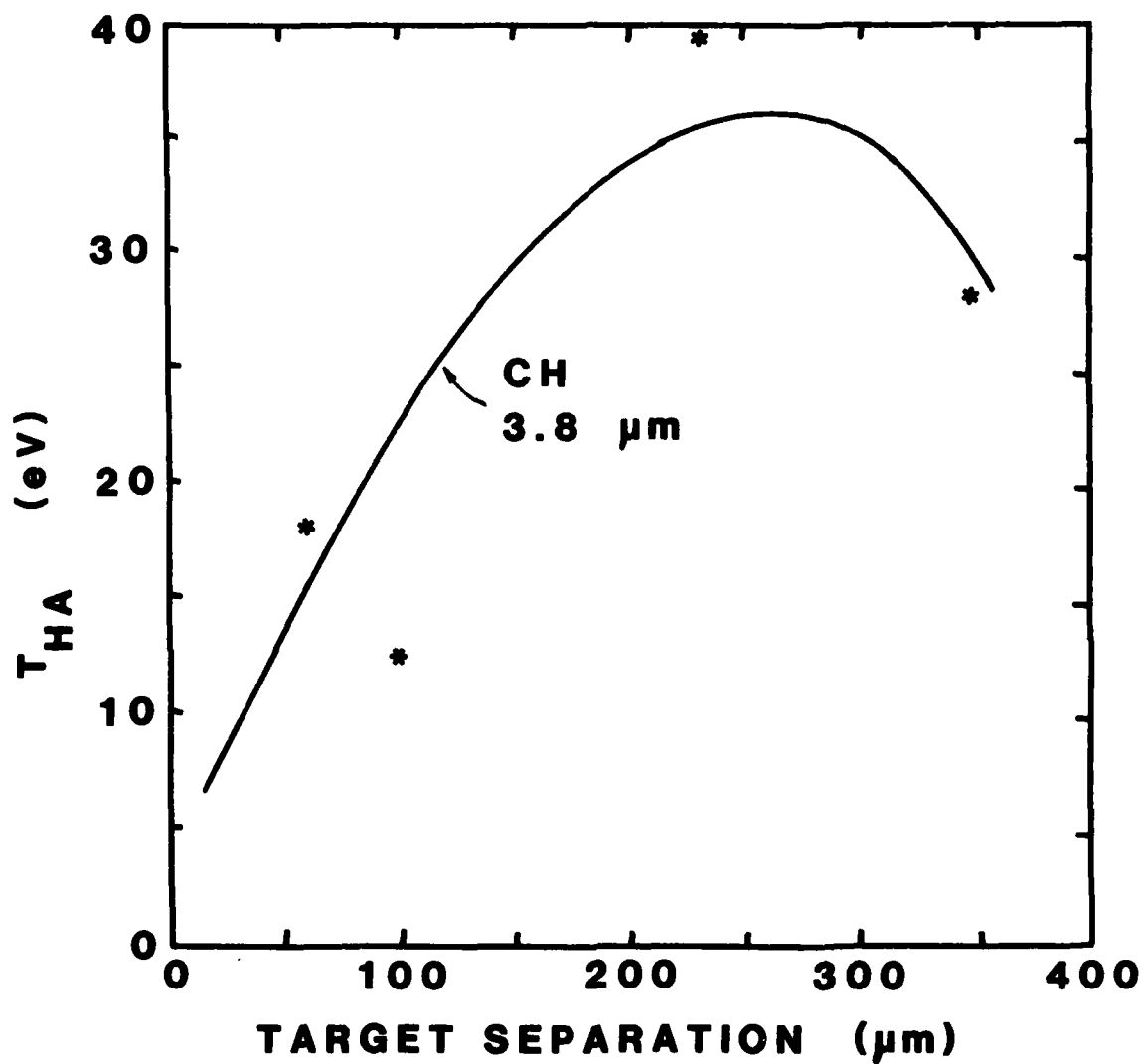


Fig. 5 — Target internal temperature from the HA-target technique as a function of the initial-target to HA separation distance. Note, the initial increase and later decline of target temperature with separation.

In summary, we have demonstrated a new diagnostic of the internal thermodynamic properties of highly-accelerated targets. The results corroborate rear-surface temperature measurements of the same targets obtain using time-resolved optical pyrometry. Thus, the relatively low target preheat values found in moderate-irradiance ablative acceleration experiments,^{1,4,11} are confirmed by an independent method. This experimental method also yields the internal pressure in these targets, which could be compared with shock wave measurements. Alternately, if temperature information is known from another source, the effective ionization state of the dense material may be inferred.

We thank J. Grun and S. Obenschain for diagnostic assistance and E. Turbyfill, N. Nocerino and L. Seymour for technical assistance. This work was funded by the U.S. Department of Energy.

REFERENCES

1. E.A. McLean, S.H. Gold, J.A. Stamper, R.R. Whitlock, H.R. Griem, S.P. Obenschain, B.H. Ripin, S.E. Bodner, M.J. Herbst, S.J. Gitomer, and M.K. Matzen, Phys. Rev. Lett. 45, 1246 (1980).
2. For example see: R.A. Lerche, L.W. Coleman, J.W. Houghton, D.R. Speck, and E.K. Storm, Appl. Phys. Lett. 31, 645 (1977); T.H. Tan et al. Phys. Fluids 24, 754 (1981).
3. J.D. Hares, J.D. Kilkenny, M.H. Key and J.G. Lunney, Phys. Rev. Lett. 42, 1216 (1979); B. Yaakobi, I. Pelah, and J. Hoose, Phys. Rev. Lett. 37, 836 (1976).
4. S.P. Obenschain, J. Grun, B.H. Ripin and E.A. McLean, Phys. Rev. Lett. 46, 1402 (1981).
5. Ya. B. Zel'dovich and Yu. P. Raizer, Physics of Shock Waves and High Temperature Hydrodynamic Phenomena, Academic Press, NY (1966), Vol. I, p. 101-106.
6. SESAME EOS library tables were kindly provided by the Los Alamos Scientific Laboratory. Appreciation is extended also to D. Bacon who adapted the library to the NRL computer.
7. M. Widner, I. Alexeff, and W.D. Jones, Phys. Fluids 14, 795 (1971).
8. J.M. McMahon, R.P. Burns, T.H. DeRieux, R.A. Hunsicker, R.H. Lehmberg, IEEE, J. Quant. Elec. QE-17, 1629 (1981).
9. B.H. Ripin, R. Decoste, S.P. Obenschain, S.E. Bodner, E.A. McLean, F.C. Young, R.R. Whitlock, C.M. Armstrong, J. Grun, J.A. Stamper, S.H. Gold, D.J. Nagel, R.H. Lehmberg, and J.M. McMahon, Phys. Fluids 23, 1012 (1980); and 24, 990 (1981).
10. S.H. Gold and E.A. McLean, J. Appl. Phys. 53, 784 (1982).

11. B.H. Ripin, S.E. Bodner, D.G. Colombant, M.H. Emery, J.H. Gardner,
J. Grun, M.J. Herbst, R.H. Lehmberg, W.M. Manheimer, E.A. McLean, J.M.
McMahon, S.P. Obenschain, J.A. Stamper, R.R. Whitlock and F.C. Young,
Proceedings of the Conf. on Symmetry Aspects of Inertial Confinement
Fusion, Naval Research Laboratory, May 27-28, 1981 (to be published).

DATE
ILME
—8